

# Tetrazole-based, Anhydrous Proton Exchange Membranes for Fuel Cells

Min-Kyu Song, Huiping Li, Jinhuan Li, Dan Zhao, Jenghan Wang, and Meilin Liu\*

A fuel cell is an electrochemical device that can directly convert the chemical energy of fuel to electricity. Among all types of fuel cells demonstrated so far, proton exchange membrane (PEM) fuel cells are considered the best candidate for the next generation electrical vehicles.<sup>[1,2]</sup> They are also promising replacements for rechargeable batteries in portable electronic devices due to their high energy density. Although remarkable technical progress has been made in recent years, many challenges to fuel cell commercialization still remain.<sup>[3,4]</sup> Most of these difficulties are associated with the need for humidification of conventional PEMs (e.g., Nafion),<sup>[2,4,5]</sup> which limits the maximum operating temperature below the boiling point of water (i.e., 100 °C) under atmospheric pressure. This limited operating temperature (typically 60–80 °C) requires very expensive platinum catalysts, which can be readily poisoned by trace amounts of CO.<sup>[6]</sup> Additionally, hydrated membranes can suffer from degradation induced by freeze/thaw cycles (e.g., fuel cell vehicles in the winter season).<sup>[7]</sup> Also, conventional Nafion-based PEM fuel cells may not be suited for small microelectronic devices, as they require bulky and complicated water/thermal management systems.<sup>[8]</sup>

PEM fuel cells that can be operated above 100 °C under low-humidity conditions are highly desirable because expensive platinum catalysts may be replaced by abundant oxide-based catalysts and the cumbersome water management system may be eliminated or dramatically simplified.<sup>[9,10]</sup> Great efforts have been made to develop novel PEMs for fuel cells that can be operated in low humidity at high temperatures (above 100 °C), including modified Nafion,<sup>[11]</sup> alternative sulfonated polymers,<sup>[12]</sup> and heterocycle and acid based polymers.<sup>[9,13]</sup> Among them, phosphoric acid (PA) doped polybenzimidazole (PBI)-based membranes have gained the most attention due to good proton conductivity at high temperatures (150–200 °C).<sup>[14]</sup> However, PBI-based membranes show very low proton conductivity at room temperature,<sup>[9]</sup> leading to long start-up time for automotive applications. They are not suited for microelectronic devices either because of the high operating temperature. Thus, there is a need for new PEMs that have high proton conductivity and good stability in a wide temperature range (from room temperature to above 100 °C) with little humidification.

Here we report tetrazole-based PEM fuel cells operated under low humidity conditions at 20 to 120 °C. The proton

conductivity of this tetrazole-based PEM showed little dependence on humidity and temperature, ideally suited for applications in low humidity at high temperatures. Also, it is electrochemically stable in a wide range of electrical potential, a requirement of long-term stability under harsh fuel cell operating conditions. Further and in particular, fuel cells based on this PEM demonstrated excellent performance at 20 °C, and the performance increased with temperature under very dry conditions due to enhanced electrode kinetics.

As an aromatic heterocyclic compound, tetrazole (Figure 1a) with formula CH<sub>2</sub>N<sub>4</sub> consists of a five-membered ring of four nitrogen atoms and one carbon atom. Having a ring structure similar to that of imidazole (Figure 1b), it may conduct protons through either an inter- or intra- molecular proton transfer mechanism, as does imidazole. However, there are multiple advantages in using tetrazole versus imidazole. As previously reported, once a proton is transferred from one imidazole ring to another, the imidazole ring must flip before subsequent inter-molecular proton transfer can occur in the same direction. This reorientation was presumed to be the rate-determining step for long-range motion of protons in imidazole-based membranes.<sup>[15]</sup> In contrast, adjacent nitrogen atoms between tetrazole rings may act as additional proton acceptors, thus effectively promoting inter-molecular proton transfer. Intra-molecular proton transfer (tautomerization by migration of protons via a switch of a single bond with an adjacent double bond) within each tetrazole ring may also play an important role in proton transport. The difference in Pauling electronegativity between N and H is 0.8, while only 0.3 for C and H, implying protons are more loosely bound to N than to C. This leads one to expect higher intra-molecular proton transport within a tetrazole ring containing four closely located nitrogen atoms compared to an imidazole ring containing only two sparsely located nitrogen atoms. The interactions between H and each N atom along the ring are believed to be nearly the same, although there might be some differences in lengths of single and double bonds. All of these proton transfer processes may occur in a coordinated fashion. As a consequence, protons can hop from one tetrazole ring to another more effectively without flipping of rings. Our preliminary computational calculations show that the tetrazole is expected to be superior to imidazole in terms of the long-range proton transport process (Figure S2, Supporting Information). This proposed proton transfer mechanism, while plausible, is yet to be investigated through more rigorous computation and experimental measurements.

Very recently, tetrazole-based polymers have been investigated as proton exchange membranes for fuel cell applications.<sup>[16–18]</sup> For example, H<sub>3</sub>PO<sub>4</sub>-doped poly(5-vinyltetrazole)-based membranes exhibited a proton conductivity of ~0.003 S cm<sup>-1</sup> at 110 °C under dry condition.<sup>[16]</sup> Similarly,

M.-K. Song,<sup>[†]</sup> H. Li,<sup>[†]</sup> J. Li, D. Zhao, J. Wang, M. Liu  
School of Materials Science and Engineering  
Georgia Institute of Technology  
Atlanta, GA, 30332–0245, USA  
E-mail: meilin.liu@mse.gatech.edu

<sup>[†]</sup>These authors contributed equally to this work.



DOI: 10.1002/adma.201304121

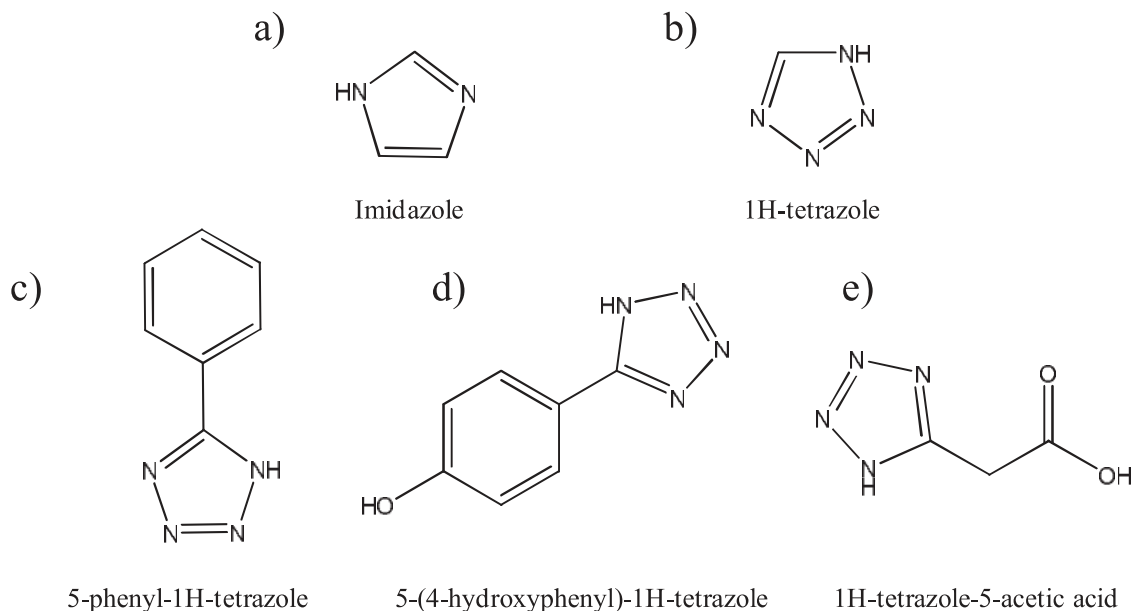


**Figure 1.** Molecular structure of a) imidazole, b) 1H-tetrazole, and 5-R-1H-tetrazole proposed in this study as new protogenic groups: c) 5-phenyl-1H-tetrazole, d) 5-(4-hydroxyphenyl)-1H-tetrazole, and e) 1H-tetrazole-5-acetic acid.

$\text{H}_3\text{PO}_4$ -doped, 5-aminotetrazole-functionalized poly(glycidyl methacrylate) membranes exhibited a good anhydrous proton conductivity of  $\sim 0.01 \text{ S cm}^{-1}$  at  $150 \text{ }^\circ\text{C}$ .<sup>[17]</sup> These results suggest the promise of tetrazole-moieties as anhydrous proton conductors, but their proton conductivities were yet to be improved further for commercially viable fuel cells. Also, successful fuel cell performance with tetrazole-based membranes has not been demonstrated thus far.

In this work, as pure tetrazoles are unstable, we propose 5-R-1H-tetrazoles as new protogenic groups. Figure 1c, 1d, and 1e show the proposed molecular structure of 5-R-1H-tetrazole: a) 5-phenyl-1H-tetrazole, b) 5-(4-hydroxyphenyl)-1H-tetrazole, and c) 1H-tetrazole-5-acetic acid. 5-R-1H-tetrazole has a ring structure similar to that of its parent compound and imidazole, with varying substituents (R). Hence, 5-R-1H-tetrazole may conduct protons through either inter- or intra- molecular proton transfer mechanisms, as does imidazole or pure tetrazole. As shown in Table S1, 1H-tetrazole and 5R-1H-tetrazoles have smaller pKa values (or more acidic and can easily donate protons) than imidazole, which may significantly influence proton concentration in the solid electrolytes. We measured the anhydrous proton conductivity of macromonomers bearing different tetrazole derivatives: 5-phenyl-1H-tetrazole and 5-(4-hydroxyphenyl)-1H-tetrazole. As shown in Figure S3, 5-(4-hydroxyphenyl)-1H-tetrazole grafted polysiloxane showed higher anhydrous proton conductivity. Although the mechanism of conduction is not clearly understood, the different substituents (Ph vs. PhOH in this case) in 5-R-1H-tetrazole may play a vital role by donating mobile protons.

We chose 5-(4-hydroxyphenyl)-1H-tetrazole as a model compound and synthesized inorganic-organic hybrid polymer membranes using an in-situ polymerization (sol-gel) process in the presence of  $\text{H}_3\text{PO}_4$  as catalyst and dopant, and porous expanded-polytetrafluoroethylene (e-PTFE) film as

reinforcement to provide mechanical strength. The membranes were then immersed in concentrated  $\text{H}_3\text{PO}_4$  solution for free-acid doping to further increase the proton conductivity. The synthetic route to organic/inorganic polymers bearing different 5-R-1H-tetrazole pendant protogenic groups and their characterization results are shown in Figure 2 and Figure S4–8. The PEM prepared by a modified sol-gel process is sufficiently dense as shown in Figure S6. FTIR and  $^{31}\text{P}$  MAS NMR analysis results suggest that  $\text{H}_3\text{PO}_4$  might join polycondensation and be grafted to the backbone during the in-situ sol-gel process, in addition to free  $\text{H}_3\text{PO}_4$  doped by immersing as-synthesized membranes in concentrated  $\text{H}_3\text{PO}_4$  solution (Figure S7 and S8).

We measured the weight increase after the as-prepared membranes were immersed in free acid for 24 hours, followed by drying at  $120 \text{ }^\circ\text{C}$  for 48 hours. The average weight gain was about 5.2 wt%, implying that additional 5.2 wt% of PA was doped into the membranes. If the PA-doping level is defined as the molar ratio of the PA per tetrazole ring,<sup>[19]</sup> the PA-doping level of tetrazole-based membranes was estimated to be  $\sim 3.15 \text{ mol}$  and  $\sim 3.3 \text{ mol}$  of PA per mole of tetrazole ring before and after immersion in free acid. The PA-doping level of tetrazole-based membrane is still lower than those of the PBI-based membranes (e.g., 6–32 mol PA per PBI repeat unit) as reported in the literature.<sup>[19,20]</sup>

As shown in Figure 3a, the proton conductivities of PA doped tetrazole-based membranes were studied using electrochemical impedance spectroscopy (EIS) under real fuel cell conditions using  $\text{H}_2$  and  $\text{O}_2$  gas with 3 vol.% of water vapor (by passing through water kept at  $20 \text{ }^\circ\text{C}$ ). These novel membranes showed good proton conductivity:  $0.041 \text{ S cm}^{-1}$  at  $120 \text{ }^\circ\text{C}$  with relative humidity of only 1.2%. Proton conductivity decreased slightly as the temperature was reduced, but still showed greater than  $0.03 \text{ S cm}^{-1}$  at  $40 \text{ }^\circ\text{C}$  with relative humidity of 31.7%. The proton conductivity of PA-doped PBI system ranged from

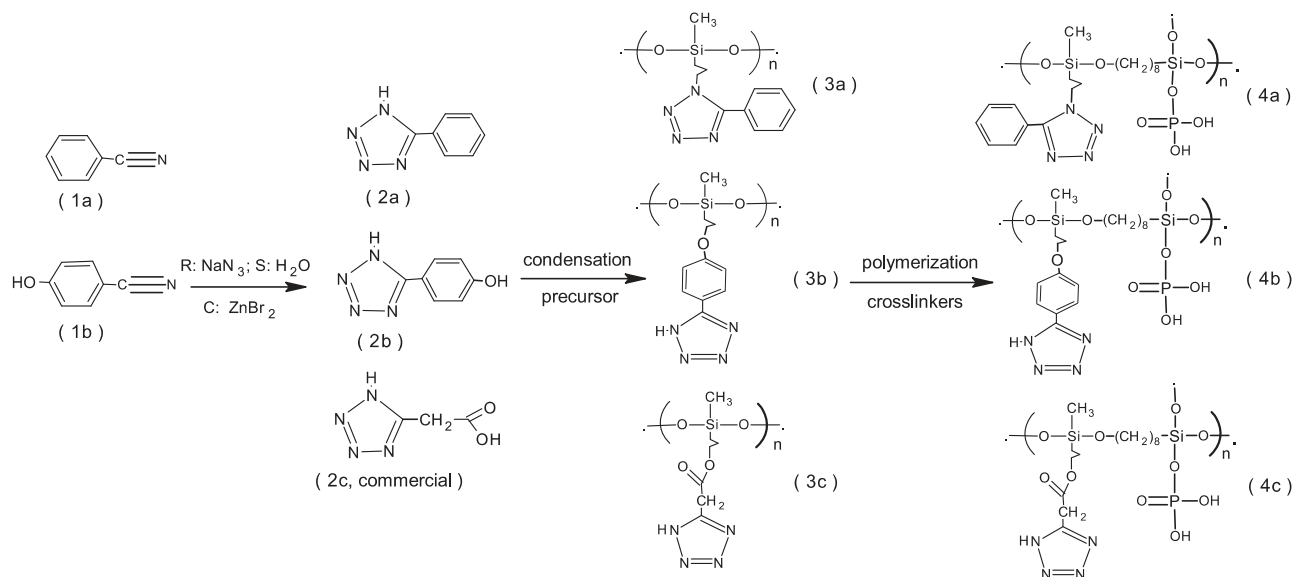


Figure 2. Proposed synthetic route to inorganic/organic hybrid polymers bearing 5-R-1H-tetrazole.

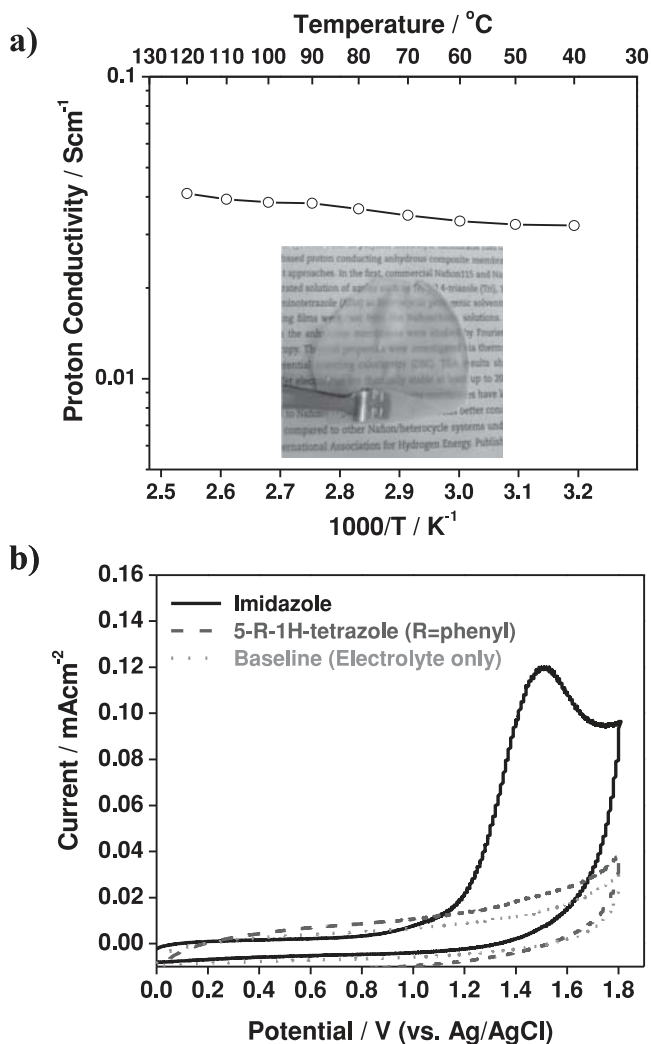
$0.04 \text{ S cm}^{-1}$  at  $190 \text{ }^\circ\text{C}$  with 6.0 mol PA/PBI to  $0.26 \text{ S cm}^{-1}$  at  $200 \text{ }^\circ\text{C}$  with 32 mol PA/PBI.<sup>[19]</sup> It is very encouraging that these new PA doped tetrazole-based membranes have good proton conductivity in a wide temperature range ( $40$  to  $120 \text{ }^\circ\text{C}$ ) under low humidity conditions. This type of fuel cells have potential for portable electronics and automotive applications, where low temperature operation is required for effective start-up and small size or light weight is vital to portability.

To study the electrochemical stability of tetrazole-based PEMs, we performed cyclic voltammetry in a typical three-electrode cell. As shown in Figure 3b, potential was swept between  $0.0$  and  $1.8 \text{ V}$  (vs. Ag/AgCl reference electrode) at a constant scan rate ( $10 \text{ mV s}^{-1}$ ) to investigate the stability of 5-R-1H-tetrazole within the operating window of fuel cells. For this purpose, 5-phenyl-1H-tetrazole was chosen because the hydroxyl group in 5-(4-hydroxyphenyl) before grafting to polysiloxane is susceptible to oxidation. The electrolyte was  $0.1 \text{ mol dm}^{-3}$  tetrabutylammonium hexafluorophosphate (TBAPF<sub>6</sub>) in acetonitrile ( $\text{CH}_3\text{CN}$ ) solution, contained  $5 \times 10^{-3} \text{ mol dm}^{-3}$  of 5-phenyl-1H-tetrazole, and was purged with nitrogen gas before experiments. No obvious reduction/oxidation peaks were observed in the cyclic voltammogram in a wide potential range. Similar curves were observed when the solution was purged with hydrogen and oxygen, respectively, suggesting that materials with tetrazole side group have adequate electrochemical stability under fuel cell operating conditions. In contrast, when  $5 \times 10^{-3} \text{ mol dm}^{-3}$  of imidazole was added to a solution containing the same concentration of 5-phenyl-1H-tetrazole, a large irreversible oxidation peak was observed in the range  $0.8$ – $1.8 \text{ V}$ . This implies that imidazole-based membranes may have potential stability issues under harsh fuel cell operating conditions. It is noted that imidazole may be oxidized to a C2-carbene-metal complex, either directly or after insertion of metal into the C=C double bond of an imidazole dimer as it has acidic proton in position 2. Further studies would be necessary to fully understand the electrochemical stability of imidazole. It

is expected that 2-phenylimidazole (which is the substructure of PBI) would be stable as C2 has a substituent (i.e., phenyl).

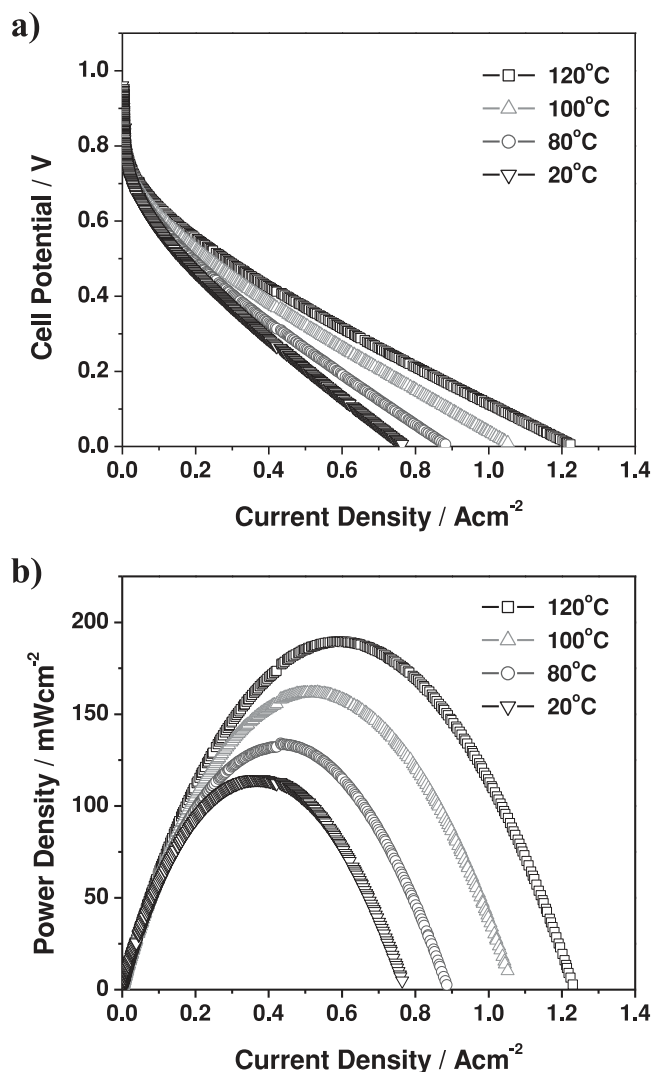
Open cell voltage (OCV) measurements and thermal gravimetric analysis (TGA) suggest that both thermal and electrochemical stability of the tetrazole-based membranes are adequate for PEM fuel cell applications at high temperatures under low humidity conditions. As shown in Figure S9, the OCVs of the tetrazole-based fuel cells were sufficiently high ( $0.89$ – $1.0 \text{ V}$ ) over a wide temperature range, suggesting that the PEM prepared by a modified sol-gel process is sufficiently dense even at temperatures above  $100 \text{ }^\circ\text{C}$  under dry conditions without significant gas crossover. The OCV of the PA-doped PBI system is typically around  $0.9 \text{ V}$  or higher at  $160 \text{ }^\circ\text{C}$  under dry conditions.

Figure 4 shows typical current-voltage and power density curves for tetrazole-based fuel cells operated at different temperatures ( $20 \text{ }^\circ\text{C}$ – $120 \text{ }^\circ\text{C}$ ) with  $\text{H}_2$  and  $\text{O}_2$  with low humidity under ambient pressure. For this performance study, it is noted that the flow rates of the reactant gases ( $\text{H}_2$  and  $\text{O}_2$ ) were intentionally kept at  $50 \text{ mL min}^{-1}$  to both the anode and the cathode (active area  $\sim 1.23 \text{ cm}^2$ ) in order to minimize the effect of mass transport limitation on performance. Tetrazole-based fuel cells showed very good performance in a wide temperature range with low humidity (the electrode microstructure is yet to be optimized). The short-circuiting current density (the current when the cell voltage was  $0 \text{ V}$ ) and the peak power density were  $\sim 770 \text{ mA cm}^{-2}$  and  $\sim 120 \text{ mW cm}^{-2}$  at  $20 \text{ }^\circ\text{C}$ , respectively. Clearly, the performance of tetrazole-based fuel cells improved with the increase of temperature even under extremely dry conditions ( $1.2\% \text{ RH}$  at  $120 \text{ }^\circ\text{C}$ ) due to enhanced kinetics of tetrazole-based electrodes in contrast to commercial Nafion-based system.<sup>[21]</sup> The peak power density was  $\sim 120 \text{ mW cm}^{-2}$  at  $20 \text{ }^\circ\text{C}$  and  $\sim 190 \text{ mW cm}^{-2}$  at  $120 \text{ }^\circ\text{C}$ . This is sufficient for many microelectronic devices. We expect that the incorporation of optimized electrodes will further enhance the performance of tetrazole-based fuel cells.



**Figure 3.** a) Proton conductivity of PA doped tetrazole-based membranes measured at different temperature with dry  $\text{H}_2$  and  $\text{O}_2$  under ambient pressure. Inset shows the image of a flexible inorganic-organic hybrid membrane bearing 5-(4-hydroxyphenyl)-1H-tetrazole. b) Electrochemical stability of 5-R-1H-tetrazole (R = phenyl) and imidazole under simulated fuel cell operating conditions.

It is noted that the demonstrated performance (e.g.,  $\sim 160 \text{ mA cm}^{-2}$  at 0.6 V at 120 °C, 1.2% RH) of the tetrazole-based membrane is inferior to that (e.g.,  $\sim 1000 \text{ mA cm}^{-2}$  at 0.6 V at 65 °C, 100% RH) of commercial, fully humidified Nafion-based membranes.<sup>[22]</sup> However, the performance of Nafion-based fuel cells decreases dramatically with temperature because Nafion is not functional under dry or low humidity conditions.<sup>[23]</sup> Many attempts have been made to overcome the drawbacks from the dry operation by increasing operation pressure to 3–5 atm in a pressurizing system;<sup>[24]</sup> however, a complex, pressurized fuel cell system may not be suited for automotive applications. It is also noted that the peak power density (e.g.,  $\sim 190 \text{ mW cm}^{-2}$  at 120 °C, 1.2% RH) of the tetrazole-based membrane with a PA-doping level of  $\sim 3.3$  mol PA per tetrazole ring is lower than those of the PBI-based membranes with PA-doping levels of 6–32 mol PA per PBI repeat unit.<sup>[19,20]</sup> For example, the highest



**Figure 4.** Performance of PA doped tetrazole-based fuel cells operated at different temperature with dry  $\text{H}_2$  and  $\text{O}_2$  under ambient pressure: a)  $I$ - $V$  curve and b) power density.

power output ( $\sim 900 \text{ mW cm}^{-2}$  at 160 °C) was reported for the membranes with 32 mol PA per PBI repeat unit.<sup>[19]</sup> Although commercial PBI-based membrane (from PEMEAS Fuel Cell Technologies) showed higher performance (e.g., the peak power density increased from  $\sim 360 \text{ mW cm}^{-2}$  at 120 °C to  $\sim 540 \text{ mW cm}^{-2}$  at 200 °C) at high temperatures (120–200 °C),<sup>[25]</sup> their performance at room temperature is unacceptable for microelectronics and automotive applications.<sup>[9]</sup> It also requires a long start-up time, making it necessary to have an auxiliary power unit. In contrast, the tetrazole-based fuel cells offer impressive performance over a wide temperature range with little humidification under ambient pressure.

The high proton conductivity under low humidity conditions of new membranes can be ascribed to the following five attributes: First, the grafted 5-R-1H-tetrazole rings can effectively transport protons between adjacent nitrogen atoms through both inter- and intra-molecular proton transfers,

without requiring water as a proton carrier. Second, acid groups ( $-\text{PO}_3\text{H}_2$ ) grafted onto hybrid inorganic-organic polymer backbones shall further increase proton conductivities. The schematics of proposed proton conduction mechanism with and without phosphonate groups are shown in Figure S10. Third, the different substituents in 5-R-1H-tetrazole may play a vital role by donating an extra proton. Fourth, 5-R-1H-tetrazoles have much smaller pKa values than imidazole (pKa1 = 7.18, pKa2 = 14.52); for instance, 5-phenyl-1H-tetrazole (pKa1 = -2.88, pKa2 = 4.50) is much more acidic, implying it can more easily donate protons. Finally, free  $\text{H}_3\text{PO}_4$  acids doped into tetrazole-based membranes would further enhance the proton conduction without water by forming a long chain of intermolecular hydrogen bonds.

In summary, we have demonstrated a new class of proton conducting, tetrazole-based inorganic-organic hybrid membranes for fuel cells. The PA doped tetrazole-based membrane has high proton conductivity over a wide temperature range (20–120 °C) under very low humidity conditions. Moreover, PEMs containing tetrazoles are stable over a wide potential range, implying excellent electrochemical stability under harsh fuel cell operating conditions. Our results suggest that high power density can be achieved under low humidity conditions at low temperatures. Although these initial results are encouraging, additional research is necessary to investigate proton conduction mechanisms and enhance fuel cell performance. It is anticipated that this novel membrane may dramatically simplify fuel cell systems and facilitate the commercialization of fuel cells for microelectronics and zero emission vehicles. It may also open up new applications which require power sources operable over a wide temperature range without cumbersome humidification and pressurization.

## Experimental Section

**Preparation of Tetrazole-Based Membranes:** We synthesized several 5-R-1H-tetrazoles by click chemistry in a one-pot reactor using aqueous solvents (please see the supplementary information for details).<sup>[26]</sup> We obtained tetrazole-bearing polymers by grafting 5-R-1H-tetrazoles to a polysiloxane backbone through nucleophilic substitution. We then fabricated novel polymer membranes using the in-situ polymerization (sol-gel) process under the presence of phosphoric acid as the catalyst and the dopant, and provided mechanical strength via the reinforcement of expanded-polytetrafluoroethylene (e-PTFE) film. The membranes were then immersed in concentrated  $\text{H}_3\text{PO}_4$  solution for 1 day (for free-acid doping) at 20 °C to increase the proton conductivity further. The phosphoric acid-doped tetrazole membranes were taken out, wiped-out and dried inside the oven at 120 °C for 2–3 days. Typical membrane thickness was 50–80  $\mu\text{m}$ . The structures of these polymers were characterized using IR and NMR. The detailed process is described in the supporting information.

**Electrochemical Characterization:** Proton conductivities of PA doped tetrazole-based membranes were measured in dry  $\text{H}_2$  and  $\text{O}_2$  by the EIS method. The potential was controlled by potentiostat (Solartron, SI 1286), and the EIS analysis was carried out with a frequency response analyzer (Solartron, SI 1255) under the influence of 10 mV ac voltage in the frequency range 0.01 Hz to 1 MHz.

To study the electrochemical stability of polymer with tetrazole side group, cyclic voltammetry was performed in a typical three-electrode at room temperature. A platinum disk (geometric area = 0.196  $\text{cm}^2$ ) and a platinum wire were used as working electrode and counter electrode, respectively. Potential was swept from 0.0–1.8 V (vs.  $\text{Ag}/\text{AgCl}$  as

reference electrode) with constant scan speed (10  $\text{mV s}^{-1}$ ) to investigate the stability of 5-phenyl-1H-tetrazole within the operating window of fuel cells. The 0.1  $\text{mol dm}^{-3}$  of TBAPF<sub>6</sub> in  $\text{CH}_3\text{CN}$  solution was used as electrolyte. It contained  $5 \times 10^{-3}$   $\text{mol dm}^{-3}$  of 5-phenyl-1H-tetrazole and was purged with nitrogen gas prior to the experiments.

To measure the performance of tetrazole-based fuel cells under real fuel cell conditions, gas diffusion electrodes (GDEs) were fabricated by mixing a suitable amount of macromonomers bearing 5-(4-hydroxyphenyl)-1H-tetrazole with commercial 40% Pt/C catalysts (1:10 w/w) in the presence of  $\text{H}_3\text{PO}_4$  (0.5g for 25 $\text{cm}^2$ ) as catalyst and dopant in an ethanol/methanol mixture (1:1 v/v) for two hours, then casting this catalyst ink onto a commercial gas diffusion layer (GDL, E-TEK) with a size of 5 cm  $\times$  5 cm (i.e., 25  $\text{cm}^2$ ). The loading amount of Pt was kept at 1 $\text{mg}/\text{cm}^2$ . After being dried for 3–4 days at 20 °C and additional 2–3 days at 120 °C inside the oven, the electrode was cut using a puncher of  $\frac{1}{2}$  inch (i.e., 12.7 mm) diameter. The membrane-electrode-assembly (MEA) was fabricated by pressing two GDEs (diameter  $\sim$ 12.7 mm) onto one novel membrane (diameter  $\sim$ 40 mm) at 120 °C under a pressure of 250  $\text{kg cm}^{-2}$ . Thus, the active area of MEA was 1.23  $\text{cm}^2$  for both the anodes and cathodes. For the evaluation of fuel cell performances, dry  $\text{H}_2$  and  $\text{O}_2$  gas was used, wet to just 3 vol.% of water by passing through the water maintained at 20 °C. Based on the vapor pressure of water, relative humidity (%) was estimated as 1.2, 2.3, 4.9, 11.7, and 31.7% at 120, 100, 80, 60, and 40 °C, respectively.

## Supporting Information

Supporting Information is available from the Wiley Online Library or from the author.

## Acknowledgements

This material is based upon work supported as part of the Heterogeneous Functional Materials (HetroFoaM) Center, an Energy Frontier Research Center funded by the U.S. Department of Energy, Office of Science, Office of Basic Energy Sciences under Award Number DE-SC0001061.

Received: August 16, 2013

Revised: October 4, 2013

Published online: November 27, 2013

- [1] M. Winter, R. J. Brodd, *Chem. Rev.* **2004**, *104*, 4245.
- [2] K. D. Kreuer, *J. Membr. Sci.* **2001**, *185*, 29.
- [3] a) M. Schuster, T. Rager, A. Noda, K. D. Kreuer, J. Maier, *Fuel Cells* **2005**, *5*, 355; b) D. Zhao, J. Li, M.-K. Song, B. Yi, H. Zhang, M. Liu, *Adv. Energy Mater.* **2011**, *1*, 203; c) M. Rikukawa, K. Sanui, *Prog. Polym. Sci.* **2000**, *25*, 1463; d) R. Borup, J. Meyers, B. Pivovar, Y. S. Kim, R. Mukundan, N. Garland, D. Myers, M. Wilson, F. Garzon, D. Wood, P. Zelenay, K. More, K. Stroh, T. Zawodzinski, J. Boncella, J. E. McGrath, M. Inaba, K. Miyatake, M. Hori, K. Ota, Z. Ogumi, S. Miyata, A. Nishikata, Z. Siroma, Y. Uchimoto, K. Yasuda, K.-i. Kimijima, N. Iwashita, *Chem. Rev.* **2007**, *107*, 3904.
- [4] M. A. Hickner, H. Ghassemi, Y. S. Kim, B. R. Einsla, J. E. McGrath, *Chem. Rev.* **2004**, *104*, 4587.
- [5] a) M.-K. Song, X. Zhu, M. Liu, *J. Power Sources* **2013**, *241*, 219; b) P. Mustarelli, E. Quartarone, S. Grandi, A. Carollo, A. Magistris, *Adv. Mater.* **2008**, *20*, 1339; c) G. Alberti, M. Casciola, L. Massinelli, B. Bauer, *J. Membr. Sci.* **2001**, *185*, 73; d) C. Yang, P. Costamagna, S. Srinivasan, J. Benziger, A. B. Bocarsly, *J. Power Sources* **2001**, *103*, 1.

- [6] Q. Li, R. He, J. O. Jensen, N. J. Bjerrum, *Chem. Mat.* **2003**, *15*, 4896.
- [7] S. Kim, M. M. Mench, *J. Power Sources* **2007**, *174*, 206.
- [8] R. K. Ahluwalia, X. Wang, *J. Power Sources* **2008**, *177*, 167.
- [9] Q. Li, R. He, J. O. Jensen, N. J. Bjerrum, *Fuel Cells* **2004**, *4*, 147.
- [10] S. U. Celik, A. Bozkurt, S. S. Hosseini, *Prog. Polym. Sci.* **2012**, *37*, 1265.
- [11] a) M. Doyle, S. K. Choi, G. Proulx, *J. Electrochem. Soc.* **2000**, *147*, 34; b) K. T. Adjemian, S. J. Lee, S. Srinivasan, J. Benziger, A. B. Bocarsly, *J. Electrochem. Soc.* **2002**, *149*, A256; c) P. Dimitrova, K. A. Friedrich, U. Stimming, B. Vogt, *Solid State Ionics* **2002**, *150*, 115.
- [12] J. A. Kerres, *J. Membr. Sci.* **2001**, *185*, 3.
- [13] K. D. Kreuer, A. Fuchs, M. Ise, M. Spaeth, J. Maier, *Electrochim. Acta* **1998**, *43*, 1281.
- [14] a) J. S. Wainright, J. T. Wang, D. Weng, R. F. Savinell, M. Litt, *J. Electrochem. Soc.* **1995**, *142*, L121; b) M. F. H. Schuster, W. H. Meyer, M. Schuster, K. D. Kreuer, *Chem. Mat.* **2004**, *16*, 329; c) R. Bouchet, E. Siebert, *Solid State Ionics* **1999**, *118*, 287; d) R. H. He, Q. F. Li, G. Xiao, N. J. Bjerrum, *J. Membr. Sci.* **2003**, *226*, 169; e) Q. Li, R. He, J. O. Jensen, N. J. Bjerrum, *Fuel Cells* **2004**, *4*, 147; f) Q. Li, J. O. Jensen, R. F. Savinell, N. J. Bjerrum, *Prog. Polym. Sci.* **2009**, *34*, 449; g) Y. L. Ma, J. S. Wainright, M. H. Litt, R. F. Savinell, *J. Electrochem. Soc.* **2004**, *151*, A8; h) J. T. Wang, R. F. Savinell, J. Wainright, M. Litt, H. Yu, *Electrochim. Acta* **1996**, *41*, 193.
- [15] W. Münch, K.-D. Kreuer, W. Silvestri, J. Maier, G. Seifert, *Solid State Ionics* **2001**, *145*, 437.
- [16] H. Pu, J. Wu, D. Wan, Z. Chang, *J. Membr. Sci.* **2008**, *322*, 392.
- [17] S. Ü. Çelik, A. Bozkurt, *Eur. Polym. J.* **2008**, *44*, 213.
- [18] a) U. Sen, S. Ünügür Çelik, A. Ata, A. Bozkurt, *Int. J. Hydrogen Energy* **2008**, *33*, 2808; b) Ş. Özden, S. Ü. Çelik, A. Bozkurt, *Electrochim. Acta* **2010**, *55*, 8498; c) S. Ü. Çelik, A. Bozkurt, *Solid State Ionics* **2011**, *199*, 1; d) S. Ü. Çelik, S. Coşgun, Ü. Akbey, A. Bozkurt, *Ionics* **2012**, *18*, 101.
- [19] L. Xiao, H. Zhang, E. Scanlon, L. S. Ramanathan, E.-W. Choe, D. Rogers, T. Apple, B. C. Benicewicz, *Chem. Mat.* **2005**, *17*, 5328.
- [20] a) Y.-L. Ma, J. S. Wainright, M. H. Litt, R. F. Savinell, *J. Electrochem. Soc.* **2004**, *151*, A8; b) L. Qingfeng, H. A. Hjuler, N. J. Bjerrum, *J. Appl. Electrochem.* **2001**, *31*, 773.
- [21] Y. Tang, J. Zhang, C. Song, H. Liu, J. Zhang, H. Wang, S. Mackinnon, T. Peckham, J. Li, S. McDermid, P. Kozak, *J. Electrochem. Soc.* **2006**, *153*, A2036.
- [22] D. E. Curtin, R. D. Lousenberg, T. J. Henry, P. C. Tangeman, M. E. Tisack, *J. Power Sources* **2004**, *131*, 41.
- [23] J. Zhang, Y. Tang, C. Song, X. Cheng, J. Zhang, H. Wang, *Electrochim. Acta* **2007**, *52*, 5095.
- [24] a) P. Staiti, A. S. Aricò, V. Baglio, F. Lufrano, E. Passalacqua, V. Antonucci, *Solid State Ionics* **2001**, *145*, 101; b) P. Costamagna, C. Yang, A. B. Bocarsly, S. Srinivasan, *Electrochim. Acta* **2002**, *47*, 1023; c) C. Yang, S. Srinivasan, A. S. Arico, P. Creti, V. Baglio, V. Antonucci, *Electrochem. Solid-State Lett.* **2001**, *4*, A31.
- [25] J. Zhang, Y. Tang, C. Song, J. Zhang, *J. Power Sources* **2007**, *172*, 163.
- [26] a) Z. P. Demko, K. B. Sharpless, *J. Org. Chem.* **2001**, *66*, 7945; b) Z. Yu, X. Wang, Y. Feng, X. Zhong, *Inorg. Chem. Commun.* **2004**, *7*, 492.

